

Highly Efficient Storage of 25-Dimensional Photonic Qudit in a Cold-Atom-Based Quantum Memory

Ming-Xin Dong^{1,2,3,4}, Wei-Hang Zhang^{1,2}, Lei Zeng^{1,2}, Ying-Hao Ye^{1,2}, Da-Chuang Li^{4,*}, Guang-Can Guo^{1,2,3}, Dong-Sheng Ding^{1,2,3,†} and Bao-Sen Shi^{1,2,3,‡}

¹Key Laboratory of Quantum Information, University of Science and Technology of China, Hefei, Anhui 230026, China

²Synergetic Innovation Center of Quantum Information and Quantum Physics, University of Science and Technology of China, Hefei, Anhui 230026, China

³Hefei National Laboratory, University of Science and Technology of China, Hefei 230088, China

⁴School of Physics and Materials Engineering, Hefei Normal University, Hefei, Anhui 230601, China



(Received 25 December 2022; accepted 16 November 2023; published 15 December 2023)

Building an efficient quantum memory in high-dimensional Hilbert spaces is one of the fundamental requirements for establishing high-dimensional quantum repeaters, where it offers many advantages over two-dimensional quantum systems, such as a larger information capacity and enhanced noise resilience. To date, it remains a challenge to develop an efficient high-dimensional quantum memory. Here, we experimentally realize a quantum memory that is operational in Hilbert spaces of up to 25 dimensions with a storage efficiency of close to 60% and a fidelity of $84.2 \pm 0.6\%$. The proposed approach exploits the spatial-mode-independent interaction between atoms and photons which are encoded in transverse-size-invariant vortex modes. In particular, our memory features uniform storage efficiency and low crosstalk disturbance for 25 individual spatial modes of photons, thus allowing the storing of qudit states programmed from 25 eigenstates within the high-dimensional Hilbert spaces. These results have great prospects for the implementation of long-distance high-dimensional quantum networks and quantum information processing.

DOI: 10.1103/PhysRevLett.131.240801

Introduction.—Quantum memories [1,2] that enable quantum state storage and its on-demand retrieval are essential requirements for quantum-repeater-based quantum communication networks [3,4] and scalable quantum computation [5]. High storage efficiency [6–8] plays an important role in preserving quantum information and realizing error correction in linear optical quantum computation [9]. Although quantum memory has been widely demonstrated in conventional two-dimensional (or qubit) quantum systems, it is highly desirable to realize a high-dimensional quantum memory since manipulating a photon in a high-dimensional Hilbert space, i.e., qudit, provides many advantages over the qubit systems in quantum information processing. For example, qudits enable networks to carry more information and increase their channel capacity via superdense coding in quantum communication [10–12]; for quantum cryptography, it has been shown that qudits can provide a more secure flux of information against eavesdroppers [13–16] since the upper bound of limited cloning fidelity given by $F_{\text{clon}}^d = 1/2 + 1/(d + 1)$ scales inversely with the dimension [10], and they also feature a better resilience to noise [17,18]. Moreover, qudit systems allow the simplification of quantum logic gates [19] and permit the enhanced fault tolerance [20] in quantum computation. In this regard, the capability to sufficiently store the qudit resources with high efficiency is of crucial importance for

constituting high-dimensional networks so as to distribute high-capacity information in long-distance quantum communication and facilitate quantum computation.

Qubit memories have been widely demonstrated in many schemes that usually encode photons in polarization [6,7,21–23] degrees of freedom (d.o.f.). However, such d.o.f. can only support the two-dimensional encodings involved with the quantum memory operation. To build up a qudit memory that can store high-dimensional information, alternative d.o.f., such as time bin [24–27], and which path [28–31], have been proposed in a variety of physical systems. In particular, an energy-time entanglement with multiple temporal modes in rare-earth-doped solid memory [24] and a multiple path memory using Duan-Lukin-Cirac-Zoller protocol [32] advance the development of multi-mode memory. In addition, the photonic transverse spatial mode, e.g., orbital angular momentum mode [33–41], has attracted rapidly growing interest because of its advance of inherent infinite dimensionality. The storage of these spatial qudit states with an efficiency of 20% using the electromagnetically induced transparency (EIT) scheme [42] and efficiency of approximately 30% through the off-resonant Raman protocol [39,43,44] have been reported. However, to date, the effective quantum memory with high efficiency, e.g., above 50%, is limited to two dimensions [6,7]. The implementation of quantum memories both having high

efficiency and supporting high dimensions is highly desirable but remains an open challenge.

There are two main challenges to realizing efficient high-dimensional quantum memories. The first is to establish a uniform light-matter interface to achieve identical efficiencies for different spatial modes. The imbalanced storage efficiencies in storing different spatial modes will significantly degrade the storage fidelity of the qudit state with the increase of dimensionality. Taking the experiment using the Laguerre-Gaussian (LG) mode as a case in point, the rapid scaling of the mode waist in \sqrt{m} (m is the number of modes) [38] will lead to significant differences in light-matter interactions for different modes, thus largely limiting its applicability in higher-dimensional quantum storage. The second challenge is to constitute a highly efficient storage medium capable of storing as many multiple modes as possible [45]. To achieve this, one needs to take into account several physical parameters simultaneously in the storage process, including the transverse spatial extent of the storage medium, the waist size of the input modes, and the optical depth (OD) of the medium [7,46]. Therefore, the uniform and efficient storage of a large number of modes is technically challenging.

Here, we demonstrate a high-dimensional quantum memory working up to a 25-dimensional Hilbert space with a storage efficiency of close to 60%, using the EIT protocol [47–52] in a laser-cooled atomic ensemble. By constituting a highly efficient spatial-mode-independent light-matter interface where photons are encoded in a unique perfect optical vortex (POV) mode [53] with invariant transverse size, we are able to store a 25-dimensional qudit by mapping it onto the 25 balanced spatial modes at the center of the storage medium, and coherently retrieve these components with identical efficiencies via a control laser. The demonstrated high-dimensional quantum memory with high efficiency herein is promising for high-capacity quantum information processing.

Model and experimental setup.—Our memory scheme based on spatial-mode-independent light-matter interaction is involved with a three-level Λ -type atomic system, where the signal field (with a Rabi frequency Ω_p) drives the level $|1\rangle$ to $|3\rangle$, and the control field (with a Rabi frequency Ω_c) drives the level $|2\rangle$ to $|3\rangle$ (Fig. 1, dashed circle). The dynamical evolution of the probe field under the slowly varying envelope approximation can be described by the Maxwell equation as follows:

$$\left[\frac{1}{c} \frac{\partial}{\partial t} + \frac{\partial}{\partial z} \right] \Omega_p = i \frac{D_{\text{eff}} \Gamma}{2L} \sigma_{31}, \quad (1)$$

where Γ denotes the decay rate of $|3\rangle$, L is the length of the medium, and σ_{31} represents the atomic coherence between levels $|1\rangle$ and $|3\rangle$. $D_{\text{eff}} \propto N_{\text{tr}} g_{31} L$ represents the effective OD of an atomic ensemble, where we define an effective atomic density N_{tr} while considering a structured light field

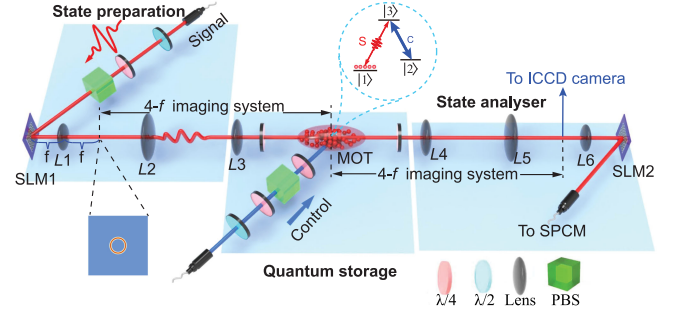


FIG. 1. Schematic experimental setup. The qudit signal encoded in POV mode via SLM 1 and lens $L1$ is mapped into the atomic ensemble for subsequent storage. Here, the signal and control fields are both circularly polarized (σ^+), and the control field is beam expanded to have a waist of 4 mm to completely cover the signal field at the center of medium.

interacts with the storage medium in the transverse orientation. g_{31} represents the photon-atom coupling coefficient between $|1\rangle$ and $|3\rangle$. It can be observed from Eq. (1) that D_{eff} significantly affects the performance of storage, and we derive the numerical relation between the storage efficiency and OD by solving the Maxwell-Bloch equations [53].

For a spatial multimode quantum memory, it is necessary to take into account the effective light-matter interaction volume for different spatial modes. Here, we focus on the coupling of the structure field with the storage medium in the cross section, because the transverse extent of the storage medium is a crucial parameter in determining the capacity of multimode memory [45]. We assume the atomic ensemble with a Gaussian distribution of the density in the radial direction $N_{\text{tr}}(r) = N_0 \exp[-r^2/(2\sigma_r^2)]$. N_0 refers to the mean atomic density, and σ_r represents the half-width of the atomic ensemble [53]. In this work, we propose a scheme to establish a uniform light-matter interface for the memory of a variety of modes via interacting the photons encoded in the POV mode with the storage medium. Theoretically, such spatial modes feature identical transverse sizes for different m , and thus they are subject to the same $N_{\text{tr}}(r)$ of atoms when they undergo the storage process. The interaction strength between the desired POV modes and medium is uniform, which manifests as the same D_{eff} and ultimately contributes to the same storage efficiency for different m . Based on this mechanism, we constitute a spatial-mode-independent quantum memory for the further implementation of storage of high-dimensional quantum states.

The experimental setup for a high-dimensional quantum memory is schematically depicted in Fig. 1. The qudits encoded in each spatial mode are formed on the basis of the POV eigenstates $|\ell\rangle$ (ℓ is chosen from -12 to 12), which is accomplished by means of a Fourier transformation of the Bessel-Gaussian (BG) state. We initially prepare the BG states by projecting the attenuated coherent states at the

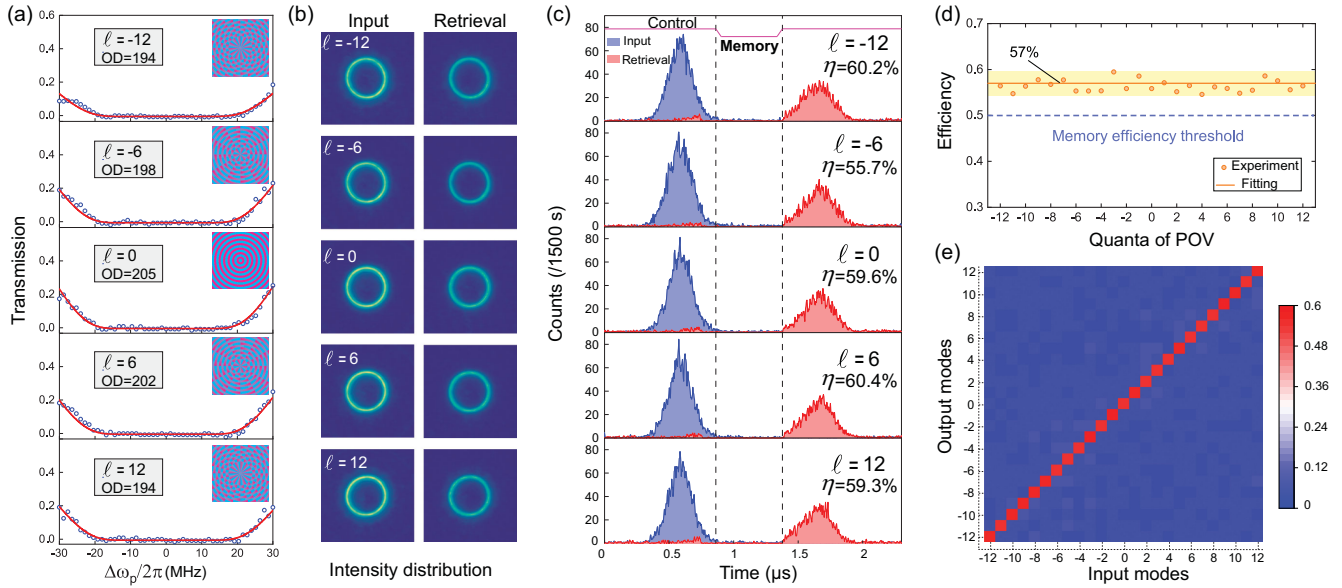


FIG. 2. Performance of spatial multimode quantum storage. (a) Measured absorption spectra for various spatial modes versus the signal detuning from the atomic resonance $|1\rangle \rightarrow |3\rangle$, where the relative computer-controlled holograms loaded on the surface of SLM1 are illustrated in the top right. (b) Transverse intensity distributions of various modes recorded at the imaging plane of the second 4- f imaging system before (left) and after (right) storage. (c) Temporal waveforms of input (blue) and retrieved (red) pulses with temporal lengths of about 500 ns for different modes. (d) Storage efficiencies versus the quanta of the POV mode. The shaded area represents the maximum fitted value that has been expected, with a span of $1(\sigma)$. (e) 25×25 input-retrieved crosstalk matrix formed by the basis set from $\ell = -12$ to 12.

single-photon level onto a phase-only spatial light modulator (SLM1) to shape the wave fronts of photons (Fig. 1, top left). The phase patterns loaded on the SLM are programmed by a combination of Bessel and Gaussian functions. Lens $L1$ acting as a Fourier transformer is then used to transform the BG states to the POV states, which are subsequently mapped into the center of the atomic medium for storage with the assistance of a carefully aligned 4- f imaging system.

Performance of multimode quantum memory.—The key to achieving multimode storage in our scheme is to exploit the mode-independent light-matter interaction. To confirm the accomplishment of this particular photon-atom interface, we first measure the absorption spectra for a variety of spatial modes, i.e., $\ell \in \{-12, -6, 0, 6, 12\}$ by scanning the detuning of signal from $-2\pi \times 30$ to $+2\pi \times 30$ MHz, as depicted in Fig. 2(a). The nearly identical OD (~ 200) for various $|\ell\rangle$ indicates that the interactions between POV photons and atoms have hardly any correlation with their mode number, thus allowing our memory to be capable of carrying multiple spatial modes simultaneously. As shown in Fig. 2(b), the spatial profiles of POV eigenstates with a mean photon number of $n = 0.5$ in the transverse orientation are detected by an intensified charge-coupled-device camera (iStar 334T series, Andor) working at the single-photon level. The calculated high values S of similarity [35] between the input and retrieved states are 99.65%, 99.63%, 99.65%, 99.61%, and 99.54% for $\ell = -12, -6, 0, 6, 12$,

respectively, implying a faithful quantum storage for POV states.

Figure 2(c) shows the temporal waveforms of the input (blue) and retrieved pulses (red) after a one-pulse-delay storage time for various spatial modes. As can be seen, the retrievals have almost the same waveforms for different inputs, providing clear evidence that our memory exhibits identical characteristics for different POV modes. To fully analyze the capacity of this spatial multimode quantum memory, we investigate the memory efficiencies of POV eigenstates across the entire range (from -12 to 12) with a step of $\Delta\ell = 1$; see Fig. 2(d). Their approximately same values at around 57% clearly illustrate that our memory enables 25 spatial-mode storage with efficiency beyond 50%. Note that the overall storage-efficiency distributions for different radial wave vectors k_r [53] in a wider mode range are shown in Fig. 3(a). Figure 2(e) gives the experimental crosstalk between the 25 orthogonal bases after retrieval. The average contrast [53] given by $C = 1/25 \sum_m C_m$ is estimated to be $92.4 \pm 1.6\%$, thereby revealing a low overlap noise between orthogonal spatial modes.

In multimode memory, the uniform storage efficiency for each POV eigenstate plays a crucial role in high-dimensional storage. We consider a high-dimensional quantum superposition state with the dimensionality of d , i.e., the so-called qudit state $|\psi\rangle_{\text{input}} = 1/\sqrt{d}(|\ell_1\rangle + |\ell_2\rangle + \dots + |\ell_d\rangle)$ as input. The retrieved state after storage can be written as

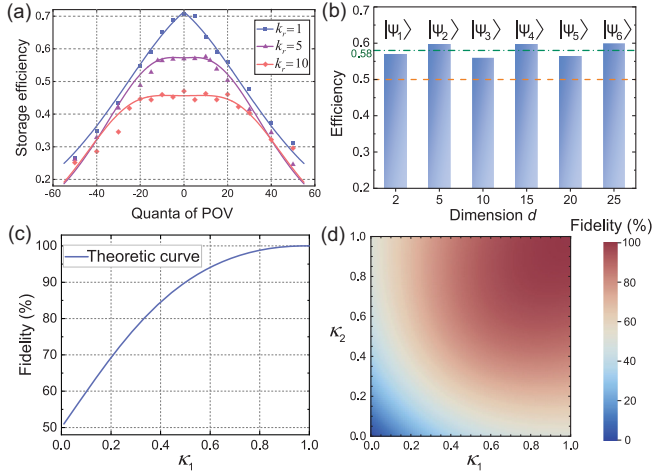


FIG. 3. Characteristics of high-dimensional storage. (a) Distributions of storage mode bandwidth for different radial wave vectors $k_r = 1, 5, 10$, where the k_r of 5 is used in the context. (b) Qudit states with $d = 2, 5, 10, 15, 20$, and 25 (see particular expressions in Ref [53]) versus storage efficiency. (c) Numerical simulation of two-dimensional fidelity as a function of the storage-efficiency uniformity κ_1 . (d) Theoretical analysis of fidelity versus κ_1 and κ_2 in the case of a qudit with $d = 3$.

$$|\psi\rangle_{\text{retrieval}} = \frac{1}{\sqrt{\sum_{m=1}^d \eta_m^2}} (\eta_1 |\ell_1\rangle + \eta_2 |\ell_2\rangle + \cdots + \eta_d |\ell_d\rangle) \quad (2)$$

where η_1, \dots, η_d denote the storage efficiency for the corresponding eigenmodes. $|\psi\rangle_{\text{retrieval}}$ can be further simplified to $\eta/\sqrt{d}(|\ell_1\rangle + |\ell_2\rangle + \cdots + |\ell_d\rangle)$ if η_1, \dots, η_d are all equal to a constant represented by η . In this case, the storage efficiency of the qudits has no dependence on the dimensionality d , as displayed by the results in Fig. 3(b). Thus, our memory allows storing arbitrarily dimensional qudits with the same efficiency even when d is up to 25.

Storage fidelity is a critical performance parameter that has to be taken into account in quantum memory. For the storage of a qudit in terms of multiple spatial modes, its fidelity is extremely sensitive to the uniformity of the storage efficiency for the internal orthogonal states. For simplicity, we consider the case of quantum states with $d = 2$, as shown in Fig. 3(c), where a parameter κ_1 is defined as the ratio of storage efficiencies between $|\ell_1\rangle$ and $|\ell_2\rangle$, i.e., $\kappa_1 = \eta_2/\eta_1$. It can be found that the imbalanced atomic storage ($\kappa_1 \ll 1$) would largely reduce the fidelity, as estimated by the formula $F = [\text{Tr}(\sqrt{\sqrt{\rho_T}\rho_{\text{retrieval}}\sqrt{\rho_T}})]^2$, where ρ_T and $\rho_{\text{retrieval}}$ represent the density matrices corresponding to the target and retrieval states. In Fig. 4(a), we reconstruct the retrieved density matrices using the quantum state tomography (QST) method for a set of qubit states constituted by the chosen eigenstates (e.g., $|0\rangle, |12\rangle$,

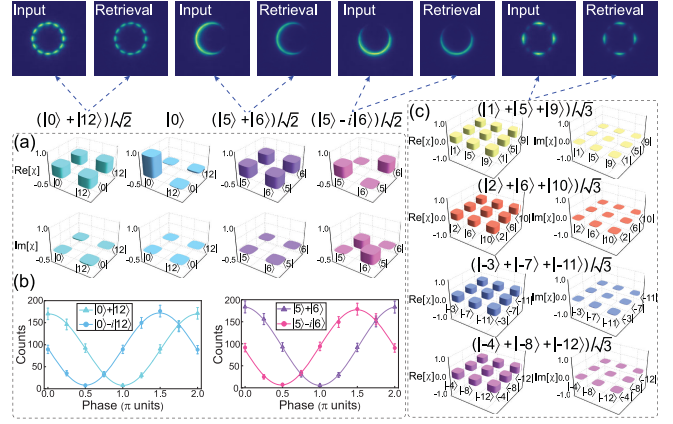


FIG. 4. Demonstration of the storage of quantum states programmed by the chosen quanta. (a) Reconstructed real and imaginary parts of density matrices of the retrieved quantum states with $d = 2$ in different subspaces. (b) Single-photon interference fringes for different states. (c) Reconstructed density matrices of the retrieved qudits with $d = 3$ in arbitrarily selected subspaces. The upper panel illustrates the spatial profiles of the corresponding quantum states before and after storage. The mean number of photons per pulse here is $n = 0.5$.

$|5\rangle, |6\rangle$ are chosen herein) after storage. The average fidelity of 95.8% without any corrections is in good agreement with the theoretical expectation, and the measured single-photon interference fringes [Fig. 4(b)] with an average visibility of 92.3% demonstrate that the coherence between two components of the qubits is well preserved during storage.

In analogy to the case of $d = 2$, Fig. 3(d) illustrates the effect of efficiency uniformity between internal modes on the fidelity for $d = 3$, where κ_2 is defined as η_3/η_1 . To obtain a high fidelity, κ_1 and κ_2 should both approach unity. In Fig. 4(c), we randomly choose three eigenvectors in the range from $|-12\rangle$ to $|12\rangle$ to prepare the high-dimensional states for storage. The high mean fidelity is measured to be 96.4% owing to $\kappa_1 \approx \kappa_2 \approx 1$. Note that these results can hardly be obtained in those experiments [38] using conventional vortex modes (e.g., the LG mode) because of the inevitable nonuniform efficiency for different spatial modes. Moreover, we characterize the retrieved state of $|\psi_2\rangle$ for $d = 5$, and the raw fidelity reaches $90.7 \pm 0.7\%$ [53] (the error bar is estimated from Poissonian statistics and using Monte Carlo simulations). All of these experimental results indicate our memory capability of storing multiple-mode-encoded qudit states programmed from 25 eigenvectors.

We now turn to study the capability of our memory to store a 25-dimensional quantum state. The main challenge of achieving the storage of a 25-dimensional qudit state is to preserve the identical memory efficiency for each mode, thus preventing the decay of coherence between 25 spatial modes during the storage process. Here, a 25-dimensional qudit state $|\Psi\rangle$ given by a coherent superposition of 25

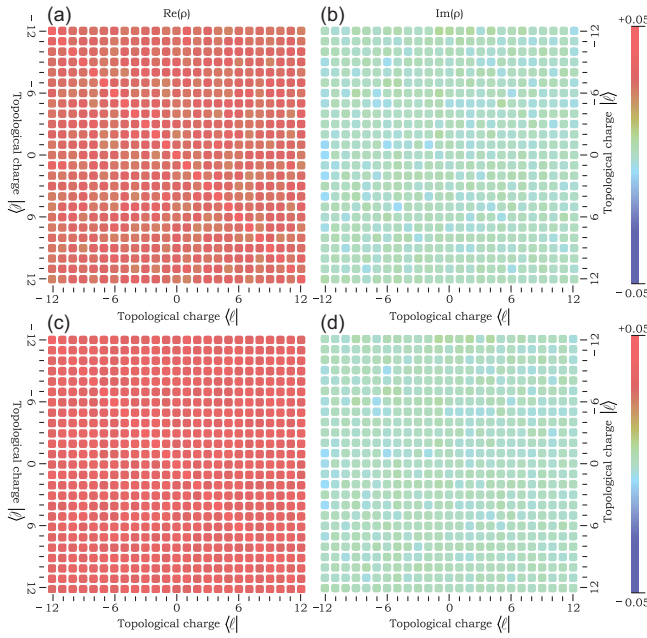


FIG. 5. Experimental realization of 25-dimensional qudit storage. The characterization of the retrieved qudit state $|\psi_6\rangle$ after the storage process by performing QST. (a),(c) and (b),(d) are the real and imaginary parts of the reconstructed density matrices for retrieved state $|\psi_6\rangle$ without and with dark counts subtraction, respectively.

individual spatial modes from $| -12\rangle$ to $|12\rangle$ is prepared for the demonstration of 25-dimensional qudit storage, which is represented as

$$|\Psi\rangle = \frac{1}{\sqrt{25}} \sum_{\ell=-12}^{+12} |\ell\rangle. \quad (3)$$

To fully characterize the retrieved state, we perform the high-dimensional QST [53,63], where the real and imaginary parts of the reconstructed density matrix without (with) background correction are plotted in the logical basis of $\{| -12\rangle, | -11\rangle, | -10\rangle, \dots, |12\rangle\}$, as shown in Figs. 5(a) and 5(b) [Figs. 5(c) and 5(d)], respectively. The raw fidelity between the retrieved states and ideal state is estimated to be $72.8 \pm 0.6\%$, where the imperfection fidelity is mainly caused by the dark counts of the detector and residual control laser leakage. After the subtraction of the dark counts, the fidelity reaches $84.2 \pm 0.6\%$, far exceeding the classical limit of 9.2% for mean photon number $n = 0.5$ with dimensionality of 25 [53], where the memory efficiency of state $|\psi_6\rangle$ equal to 60% is taken into account. Note that the residual fidelity is primarily due to the noise from the control laser and imperfections in the qudit preparation and measurement. All of the above results clearly beat the classical benchmark, thus demonstrating the quantum character of 25-dimensional memory implementation.

Conclusion.—In summary, we have experimentally demonstrated the efficient quantum storage for high-dimensional quantum states with d up to 25 using the POV modes of photons. The reported high-dimensional quantum memory with a storage efficiency of close to 60% is beneficial for quantum information applications. Remarkably, the dimensionality of this memory is scalable to as high as 100 through further optimization of the waist of POV modes [53], thus presenting a clear route to the scalability of dimensions. In addition, our multimode memory is also promising for the compatibility with fiber-based quantum information transfer systems, which are capable of spatially structured photon transmission [64,65]. The high-dimensional quantum memory demonstrated herein gives a great perspective for the practical high-capacity and long-distance quantum communication networks.

This work was supported by National Key R&D Program of China (Grant No. 2022YFA140400), Anhui Initiative in Quantum Information Technologies (Grant No. AHY020200), the National Natural Science Foundation of China (Grants No. U20A20218, No. 12204461, No. 11934013, and No. 11604322), the Major Science and Technology Projects in Anhui Province (Grant No. 202203a13010001), and Innovation Program for Quantum Science and Technology (Grant No. 2021ZD0301100).

Ming-Xin Dong and Wei-Hang Zhang contributed equally to this work.

*dachuangli@ustc.edu.cn

†dds@ustc.edu.cn

‡drshi@ustc.edu.cn

- [1] A. I. Lvovsky, B. C. Sanders, and W. Tittel, Optical quantum memory, *Nat. Photonics* **3**, 706 (2009).
- [2] N. Sangouard, C. Simon, H. De Riedmatten, and N. Gisin, Quantum repeaters based on atomic ensembles and linear optics, *Rev. Mod. Phys.* **83**, 33 (2011).
- [3] H.-J. Briegel, W. Dür, J. I. Cirac, and P. Zoller, Quantum repeaters: The role of imperfect local operations in quantum communication, *Phys. Rev. Lett.* **81**, 5932 (1998).
- [4] H. J. Kimble, The quantum internet, *Nature (London)* **453**, 1023 (2008).
- [5] P. Kok, W. J. Munro, K. Nemoto, T. C. Ralph, J. P. Dowling, and G. J. Milburn, Linear optical quantum computing with photonic qubits, *Rev. Mod. Phys.* **79**, 135 (2007).
- [6] P. Vernaz-Gris, K. Huang, M. Cao, A. S. Sheremet, and J. Laurat, Highly-efficient quantum memory for polarization qubits in a spatially-multiplexed cold atomic ensemble, *Nat. Commun.* **9**, 363 (2018).
- [7] Y. Wang, J. Li, S. Zhang, K. Su, Y. Zhou, K. Liao, S. Du, H. Yan, and S.-L. Zhu, Efficient quantum memory for single-photon polarization qubits, *Nat. Photonics* **13**, 346 (2019).
- [8] J. Guo, X. Feng, P. Yang, Z. Yu, L. Q. Chen, C.-H. Yuan, and W. Zhang, High-performance raman quantum memory

- with optimal control in room temperature atoms, *Nat. Commun.* **10**, 148 (2019).
- [9] M. Varnava, D. E. Browne, and T. Rudolph, Loss tolerance in one-way quantum computation via counterfactual error correction, *Phys. Rev. Lett.* **97**, 120501 (2006).
- [10] M. Erhard, R. Fickler, M. Krenn, and A. Zeilinger, Twisted photons: New quantum perspectives in high dimensions, *Light Sci. Appl.* **7**, 17146 (2018).
- [11] M. Erhard, M. Krenn, and A. Zeilinger, Advances in high-dimensional quantum entanglement, *Nat. Rev. Phys.* **2**, 365 (2020).
- [12] M. Krenn, M. Huber, R. Fickler, R. Lapkiewicz, S. Ramelow, and A. Zeilinger, Generation and confirmation of a (100×100) -dimensional entangled quantum system, *Proc. Natl. Acad. Sci. U.S.A.* **111**, 6243 (2014).
- [13] H. Bechmann-Pasquinucci and W. Tittel, Quantum cryptography using larger alphabets, *Phys. Rev. A* **61**, 062308 (2000).
- [14] H. Bechmann-Pasquinucci and A. Peres, Quantum cryptography with 3-state systems, *Phys. Rev. Lett.* **85**, 3313 (2000).
- [15] N. J. Cerf, M. Bourennane, A. Karlsson, and N. Gisin, Security of quantum key distribution using d -level systems, *Phys. Rev. Lett.* **88**, 127902 (2002).
- [16] S. Walborn, D. Lemelle, M. Almeida, and P. S. Ribeiro, Quantum key distribution with higher-order alphabets using spatially encoded qudits, *Phys. Rev. Lett.* **96**, 090501 (2006).
- [17] L. Sheridan and V. Scarani, Security proof for quantum key distribution using qudit systems, *Phys. Rev. A* **82**, 030301(R) (2010).
- [18] S. Ecker *et al.*, Overcoming noise in entanglement distribution, *Phys. Rev. X* **9**, 041042 (2019).
- [19] B. P. Lanyon, M. Barbieri, M. P. Almeida, T. Jennewein, T. C. Ralph, K. J. Resch, G. J. Pryde, J. L. O'Brien, A. Gilchrist, and A. G. White, Simplifying quantum logic using higher-dimensional hilbert spaces, *Nat. Phys.* **5**, 134 (2009).
- [20] E. T. Campbell, Enhanced fault-tolerant quantum computing in d -level systems, *Phys. Rev. Lett.* **113**, 230501 (2014).
- [21] D.-S. Ding, W. Zhang, Z.-Y. Zhou, S. Shi, B.-S. Shi, and G.-C. Guo, Raman quantum memory of photonic polarized entanglement, *Nat. Photonics* **9**, 332 (2015).
- [22] M. Gündoğan, P. M. Ledingham, A. Almasi, M. Cristiani, and H. De Riedmatten, Quantum storage of a photonic polarization qubit in a solid, *Phys. Rev. Lett.* **108**, 190504 (2012).
- [23] Z. Xu, Y. Wu, L. Tian, L. Chen, Z. Zhang, Z. Yan, S. Li, H. Wang, C. Xie, and K. Peng, Long lifetime and high-fidelity quantum memory of photonic polarization qubit by lifting Zeeman degeneracy, *Phys. Rev. Lett.* **111**, 240503 (2013).
- [24] A. Tiranov, S. Designolle, E. Z. Cruzeiro, J. Lavoie, N. Brunner, M. Afzelius, M. Huber, and N. Gisin, Quantification of multidimensional entanglement stored in a crystal, *Phys. Rev. A* **96**, 040303(R) (2017).
- [25] C. Simon, H. de Riedmatten, M. Afzelius, N. Sangouard, H. Zbinden, and N. Gisin, Quantum repeaters with photon pair sources and multimode memories, *Phys. Rev. Lett.* **98**, 190503 (2007).
- [26] E. Saglamyurek, N. Sinclair, J. Jin, J. A. Slater, D. Oblak, F. Bussi eres, M. George, R. Ricken, W. Sohler, and W. Tittel, Broadband waveguide quantum memory for entangled photons, *Nature (London)* **469**, 512 (2011).
- [27] C. Clausen, I. Usmani, F. Bussi eres, N. Sangouard, M. Afzelius, H. de Riedmatten, and N. Gisin, Quantum storage of photonic entanglement in a crystal, *Nature (London)* **469**, 508 (2011).
- [28] C.-W. Chou, H. de Riedmatten, D. Felinto, S. V. Polyakov, S. J. van Enk, and H. J. Kimble, Measurement-induced entanglement for excitation stored in remote atomic ensembles, *Nature (London)* **438**, 828 (2005).
- [29] D. L. Moehring, P. Maunz, S. Olmschenk, K. C. Younge, D. N. Matsukevich, L.-M. Duan, and C. Monroe, Entanglement of single-atom quantum bits at a distance, *Nature (London)* **449**, 68 (2007).
- [30] K. S. Choi, H. Deng, J. Laurat, and H. Kimble, Mapping photonic entanglement into and out of a quantum memory, *Nature (London)* **452**, 67 (2008).
- [31] L. Tian, Z. Xu, L. Chen, W. Ge, H. Yuan, Y. Wen, S. Wang, S. Li, and H. Wang, Spatial multiplexing of atom-photon entanglement sources using feedforward control and switching networks, *Phys. Rev. Lett.* **119**, 130505 (2017).
- [32] Y. Pu, N. Jiang, W. Chang, H.-X. Yang, C. Li, and L.-M. Duan, Experimental realization of a multiplexed quantum memory with 225 individually accessible memory cells, *Nat. Commun.* **8**, 15359 (2017).
- [33] M. Krenn, M. Malik, M. Erhard, and A. Zeilinger, Orbital angular momentum of photons and the entanglement of Laguerre-Gaussian modes, *Phil. Trans. R. Soc. A* **375**, 20150442 (2017).
- [34] S. Franke-Arnold, Optical angular momentum and atoms, *Phil. Trans. R. Soc. A* **375**, 20150435 (2017).
- [35] D.-S. Ding, Z.-Y. Zhou, B.-S. Shi, and G.-C. Guo, Single-photon-level quantum image memory based on cold atomic ensembles, *Nat. Commun.* **4**, 2527 (2013).
- [36] A. Nicolas, L. Veissier, L. Giner, E. Giacobino, D. Maxein, and J. Laurat, A quantum memory for orbital angular momentum photonic qubits, *Nat. Photonics* **8**, 234 (2014).
- [37] V. Parigi, V. D'Ambrosio, C. Arnold, L. Marrucci, F. Sciarrino, and J. Laurat, Storage and retrieval of vector beams of light in a multiple-degree-of-freedom quantum memory, *Nat. Commun.* **6**, 7706 (2015).
- [38] D.-S. Ding, W. Zhang, Z.-Y. Zhou, S. Shi, G.-Y. Xiang, X.-S. Wang, Y.-K. Jiang, B.-S. Shi, and G.-C. Guo, Quantum storage of orbital angular momentum entanglement in an atomic ensemble, *Phys. Rev. Lett.* **114**, 050502 (2015).
- [39] W. Zhang, D.-S. Ding, M.-X. Dong, S. Shi, K. Wang, S.-L. Liu, Y. Li, Z.-Y. Zhou, B.-S. Shi, and G.-C. Guo, Experimental realization of entanglement in multiple degrees of freedom between two quantum memories, *Nat. Commun.* **7**, 13514 (2016).
- [40] C. Wang, Y. Yu, Y. Chen, M. Cao, J. Wang, X. Yang, S. Qiu, D. Wei, H. Gao, and F. Li, Efficient quantum memory of orbital angular momentum qubits in cold atoms, *Quantum Sci. Technol.* **6**, 045008 (2021).
- [41] Y.-H. Ye, L. Zeng, M.-X. Dong, W.-H. Zhang, E.-Z. Li, D.-C. Li, G.-C. Guo, D.-S. Ding, and B.-S. Shi, Long-lived memory for orbital angular momentum quantum states, *Phys. Rev. Lett.* **129**, 193601 (2022).

- [42] D.-S. Ding, W. Zhang, Z.-Y. Zhou, S. Shi, J.-s. Pan, G.-Y. Xiang, X.-S. Wang, Y.-K. Jiang, B.-S. Shi, and G.-C. Guo, Toward high-dimensional-state quantum memory in a cold atomic ensemble, *Phys. Rev. A* **90**, 042301 (2014).
- [43] K. Reim, J. Nunn, V. O. Lorenz, B. J. Sussman, K. C. Lee, N. K. Langford, D. Jaksch, and I. A. Walmsley, Towards high-speed optical quantum memories, *Nat. Photonics* **4**, 218 (2010).
- [44] K. F. Reim, P. Michelberger, K. C. Lee, J. Nunn, N. K. Langford, and I. A. Walmsley, Single-photon-level quantum memory at room temperature, *Phys. Rev. Lett.* **107**, 053603 (2011).
- [45] A. Grodecka-Grad, E. Zeuthen, and A. S. Sørensen, High-capacity spatial multimode quantum memories based on atomic ensembles, *Phys. Rev. Lett.* **109**, 133601 (2012).
- [46] M. Cao, F. Hoffet, S. Qiu, A. S. Sheremet, and J. Laurat, Efficient reversible entanglement transfer between light and quantum memories, *Optica* **7**, 1440 (2020).
- [47] T. Chanelière, D. N. Matsukevich, S. D. Jenkins, S.-Y. Lan, T. A. B. Kennedy, and A. Kuzmich, Storage and retrieval of single photons transmitted between remote quantum memories, *Nature (London)* **438**, 833 (2005).
- [48] M. D. Eisaman, A. André, F. Massou, M. Fleischhauer, A. S. Zibrov, and M. D. Lukin, Electromagnetically induced transparency with tunable single-photon pulses, *Nature (London)* **438**, 837 (2005).
- [49] H. Zhang *et al.*, Preparation and storage of frequency-uncorrelated entangled photons from cavity-enhanced spontaneous parametric downconversion, *Nat. Photonics* **5**, 628 (2011).
- [50] H.-N. Dai *et al.*, Holographic storage of biphoton entanglement, *Phys. Rev. Lett.* **108**, 210501 (2012).
- [51] Y.-H. Chen, M.-J. Lee, I.-C. Wang, S. Du, Y.-F. Chen, Y.-C. Chen, and I. A. Yu, Coherent optical memory with high storage efficiency and large fractional delay, *Phys. Rev. Lett.* **110**, 083601 (2013).
- [52] Y.-F. Hsiao, P.-J. Tsai, H.-S. Chen, S.-X. Lin, C.-C. Hung, C.-H. Lee, Y.-H. Chen, Y.-F. Chen, I. A. Yu, and Y.-C. Chen, Highly efficient coherent optical memory based on electromagnetically induced transparency, *Phys. Rev. Lett.* **120**, 183602 (2018).
- [53] See Supplemental Material at <http://link.aps.org/supplemental/10.1103/PhysRevLett.131.240801> for the experimental details and theoretical analysis, the characterization and preparation of the POV mode, the storage efficiency distribution for a wide mode spectrum, and the high-dimensional QST method, which includes Refs. [54–62].
- [54] D. Bruß and C. Macchiavello, Optimal state estimation for d -dimensional quantum systems, *Phys. Lett. A* **253**, 249 (1999).
- [55] S. Zhang, J. F. Chen, C. Liu, S. Zhou, M. M. T. Loy, G. K. L. Wong, and S. Du, A dark-line two-dimensional magneto-optical trap of ^{85}Rb atoms with high optical depth, *Rev. Sci. Instrum.* **83**, 073102 (2012).
- [56] D. G. Grier, A revolution in optical manipulation, *Nature (London)* **424**, 810 (2003).
- [57] N. Uribe-Patarroyo, A. Fraine, D. S. Simon, O. Minaeva, and A. V. Sergienko, Object identification using correlated orbital angular momentum states, *Phys. Rev. Lett.* **110**, 043601 (2013).
- [58] H. Yan, E. Zhang, B. Zhao, and K. Duan, Free-space propagation of guided optical vortices excited in an annular core fiber, *Opt. Express* **20**, 17904 (2012).
- [59] P. Vaity and L. Rusch, Perfect vortex beam: Fourier transformation of a Bessel beam, *Opt. Lett.* **40**, 597 (2015).
- [60] M. Liu *et al.*, Broadband generation of perfect Poincaré beams via dielectric spin-multiplexed metasurface, *Nat. Commun.* **12**, 2230 (2021).
- [61] M. Fleischhauer, A. Imamoglu, and J. P. Marangos, Electromagnetically induced transparency: Optics in coherent media, *Rev. Mod. Phys.* **77**, 633 (2005).
- [62] J. Pinnell, V. Rodríguez-Fajardo, and A. Forbes, How perfect are perfect vortex beams?, *Opt. Lett.* **44**, 5614 (2019).
- [63] R. T. Thew, K. Nemoto, A. G. White, and W. J. Munro, Qudit quantum-state tomography, *Phys. Rev. A* **66**, 012303 (2002).
- [64] J. Liu, I. Nape, Q. Wang, A. Vallés, J. Wang, and A. Forbes, Multidimensional entanglement transport through single-mode fiber, *Sci. Adv.* **6**, eaay0837 (2020).
- [65] H. Cao *et al.*, Distribution of high-dimensional orbital angular momentum entanglement over a 1 km few-mode fiber, *Optica* **7**, 232 (2020).